Germanium Modifications

DOI: 10.1002/anie.200800914

A 3D Network of Four-Bonded Germanium: A Link between Open and Dense**

Ulrich Schwarz, Aron Wosylus, Bodo Böhme, Michael Baitinger, Michael Hanfland, and Yuri Grin*

Solids comprising three-dimensional networks of mainly p elements, such as intermetallic clathrates or substituted skutterudites, are currently the subject of intense investigation. New materials are sought that display novel combinations of physical characteristics.[1,2]

Elemental germanium adopts a large number of open-framework structures. At ambient pressure, covalent interactions provide sufficiently high energy barriers to impede transformations so that phase formation becomes controlled kinetically, for example in allo-germanium Ge(*oP*128), Ge(*hP*8),[3] and Ge(*cF*136). This clathrate-II-type $\square_{24}Ge_{136}$ host assembly[4] persists at temperatures up to 693 K (Figure 1). Two more germanium modifications, Ge(*tP*12) and Ge(*cI*16), can be generated by decompression.[5,6] In all these allotropes, the four-bonded atoms adopt next-neighbor distances that are similar to those of diamond-type Ge(*cF*8).

Upon pressure increases to about 10.6 GPa, Ge(*cF*8) transforms into β-Sn-type Ge(*tI*4) with (4+2) coordination (Figure 1).[7] Above 75 GPa, the so-called *Imma* phase Ge(*oI*4)[8] with (4+2+2) coordination is formed. Around 80 GPa, hexagonal primitive Ge(*hP*1)[9] with coordination number eight is stable. Upon further compression, Ge(*oC*16) adopts a crystal structure in which two types of atoms are coordinated by 10 and 11 neighbors, respectively.[10] This atomic pattern transforms at higher pressures into the hexagonal-close-packed (hcp) arrangement Ge(*hP*2) with coordination number 12.[10]

The pressure-induced structural changes of the modification Ge(*cF*136) are, to date, unexplored. The material for our study, $\square_{24}Ge_{136}$, is synthesized by mild oxidation of $Na_{12}Ge_{17}$ with HCl.[11] With increasing pressure, in situ X-ray powder diffraction indicates a continuous compression of the clathrate between ambient pressure and 12.7(5) GPa (Figure 2). In these experiments, additional diffraction lines indicate a second, new phase above 7.6(5) GPa before a third, Ge(*tI*4)-type phase starts to form at 8.3(5) GPa. Above 12.7(5) GPa, the transformation into the Ge(*tI*4) pattern is completed. With decreasing pressure, a mixture of the Ge(*tI*4)-type phase and the new phase (formed at 9.8 GPa after several days) yields nearly pristine new diffraction patterns below approximately 6 GPa (Figure 2). Pressure decrease to 1.4 GPa induces a further transition into mainly Ge(*cI*16). In these experiments, the phases may contain small amounts of hydrogen, oxygen, and sodium from the starting material. To confirm the new phase unambiguously as a germanium allotrope, a second set of measurements was performed starting with pure Ge(*tP*12). After formation of Ge(*tI*4), a stepwise pressure release down from 15.4 GPa induces the formation of the new allotrope Ge(*hR*8) mixed with Ge(*cF*8) and Ge(*tP*12) below 7 GPa (Figure 2). The volume fraction of the phases as estimated from diffraction intensities is approximately 1:2:2 at 2.4 GPa.

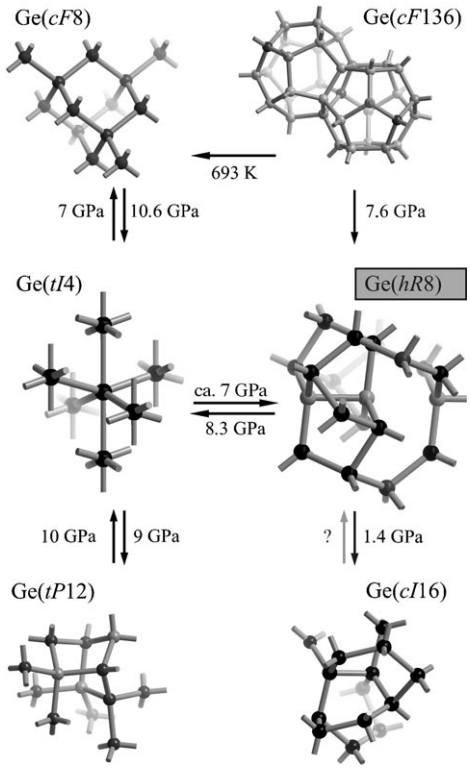

Figure 1. Germanium frameworks in elemental crystal structures. Most modifications formed at moderate pressures are related to β-Sn-like Ge(*tI*4) or to the new allotrope Ge(*hR*8) rather than to diamond-like Ge(*cF*8). The name of the new phase is shaded gray.

[*] Dr. U. Schwarz, A. Wosylus, B. Böhme, Dr. M. Baitinger, Prof. Y. Grin
Max-Planck-Institut für Chemische Physik fester Stoffe
Nöthnitzer Strasse 40, 01187 Dresden (Germany)
Fax: (+49) 351–4646–4002
E-mail: schwarz@cpfs.mpg.de
Dr. M. Hanfland
European Synchrotron Radiation Facility
6 rue Jules Horowitz, 38043 Grenoble Cedex (France)

[**] We thank Dr. Horst Borrmann, Dr. Yurii Prots, Dr. Raul Cardoso-Gil, and Steffen Hückmann for in-house X-ray diffraction experiments, Dr. Gudrun Auffermann, Ulrike Schmidt, and Anja Völzke for chemical analyses as well as Katrin Meier and Miriam Schmitt for support with the synchrotron measurements.

Supporting information for this article is available on the WWW under http://dx.doi.org/10.1002/anie.200800914.

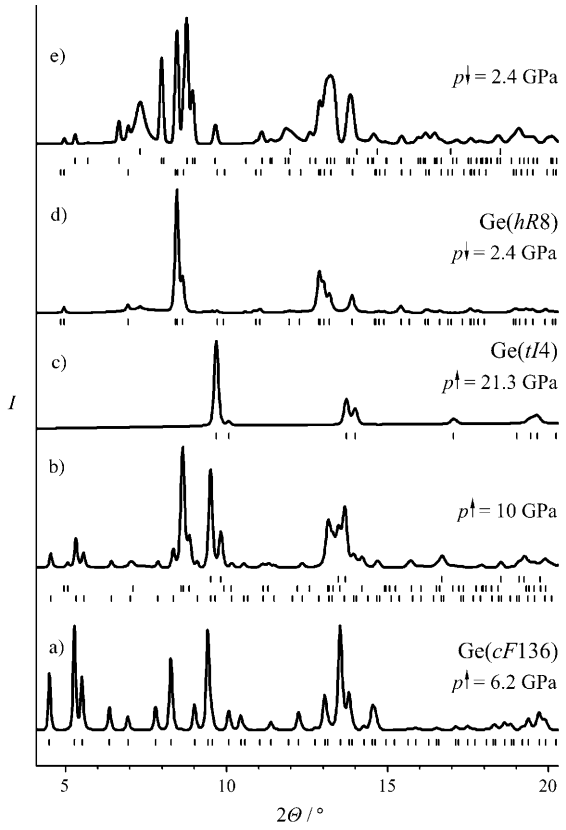

Figure 2. X-ray powder diffraction patterns at elevated pressures. Upon pressure increase (↑), the starting material Ge(*cF*136) persists up to 12.7(5) GPa (a); a phase isotypic to Ge(*hR*8) coexists with clathrate and a β-Sn-type structure between 8.3(5) GPa and 12.7(5) GPa (b). An arrangement isotypic to Ge(*tI*4) is stable at pressures exceeding 12.7(5) GPa (c). In direction of decreasing pressures (↓), the new phase is observed down to approximately 2 GPa (d). Starting from Ge(*tP*12), the new phase coexists with Ge(*cF*8) and Ge(*tP*12) upon decompression (e). Reflection positions are indicated by tick marks.

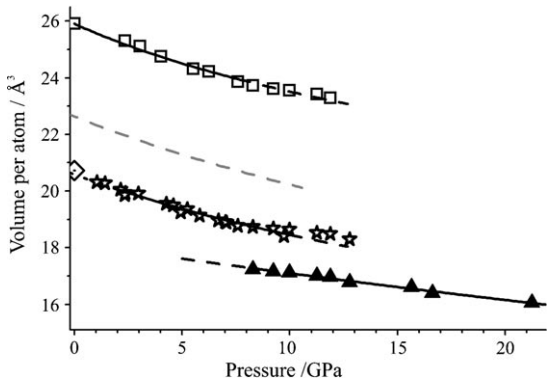

Figure 3. Atomic volumes of germanium as a function pressure: Ge(*cI*16) (diamond,[5]), Ge(*cF*136) (open squares), β-Sn-type Ge(*tI*4) (triangles), Ge(*hR*8) (stars), diamond-type Ge(*cF*8) (dashed gray line,[10]). The structural phase transitions are shown in clearly discontinuous volume changes.

Whereas the distances Ge1–Ge2 and Ge2–Ge2 change only little upon compression, a more distinct decrease is observed for the Ge1–Ge1 separations (Figure 4). The

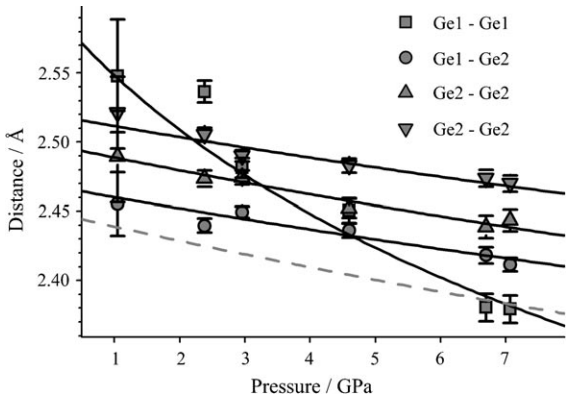

Figure 4. Pressure dependence of interatomic distances in Ge(*hR*8) The calculated values for diamond-type Ge(*cF*8) are shown as a gray dashed line. Estimated standard deviations are shown as bars.

Despite the pronounced differences in atomic volumes (Figure 3), the compressibility as revealed by the bulk moduli of the clathrate Ge(*cF*136) [$B_0 = 76(6)$ GPa, $B_0' = 6(2)$] and the new modification Ge(*hR*8) [$B_0 = 73(3)$ GPa, $B_0' = 4$] are strikingly similar to the value of 75 GPa[12] for Ge(*cF*8).

The crystal structure of Ge(*hR*8) comprises a germanium network with two types of atoms. Often such an occupation of inequivalent sites is correlated with a differentiation of the atomic coordination, for example in metals such as Mn-(*cI*58),[13] Ti(*hP*3),[14] or Ge(*oC*16)[10] and isotypic phases[15,16] as well as in more complex high-pressure modifications.[17,18] In Ge(*hR*8), both types of germanium atoms bond to four neighbors, $Ge1(Ge1)_1(Ge2)_3$ and $Ge2(Ge1)_1(Ge2)_3$. Furthermore, one type of germanium atom features a fifth contact with $d(Ge1{-}Ge1) = 3.24$ Å at 2.4 GPa. This expansion of the coordination sphere and the significantly reduced density of Ge(*hR*8) with respect to Ge(*cF*8) is reflected by an elongation of the next-neighbor distances. The spatial organization of the new allotrope may be derived from cubic Ge(*cI*16)[6] by symmetry reduction (*t*4, "translationsgleicher Übergang" of the order four[19]) and is isotypic to the high-pressure phase Si(*hR*8).[20]

pronounced anisotropy of the compressibility suggests an alternative description of the atomic arrangement. The atoms Ge2 form spirals around a 3_1 screw axis, a substructure which is similar to elemental α-Te or α-Se, Te(*hP*3) and Se(*hP*3). These one-dimensional building blocks are linked by Ge2–Ge2 contacts into a 3D host network enclosing channels along the *c* axis. The other germanium guest atoms (Ge1) form chains with alternating long and short separations in the resulting tubular voids (Figure 5). A similar structural organization is observed in the tetragonal high-pressure modifications of K-III (Rb-IV) and Sb-II (Figure 5), which exhibit incommensurate identity periods of the partial structures along the chain direction.[17]

The special partitioning of the Ge(*hR*8) crystal structure implicates dissimilar guest–guest, host–host, and host–guest interactions; therefore, the chemical bonding was analyzed by means of the electron localizability indicator (ELI[21]).

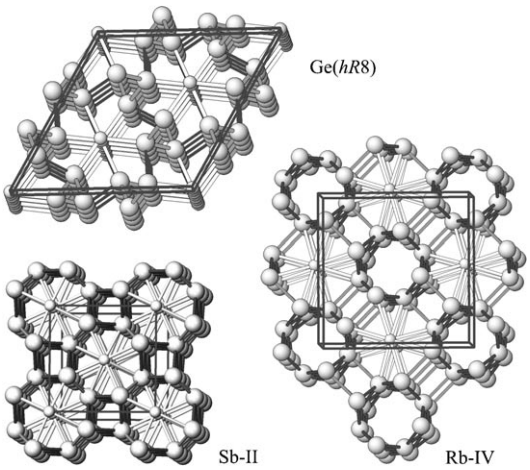

Figure 5. Atomic arrangements in the crystal structures of Ge(*hR*8) (Ge1: smaller spheres, Ge2: larger spheres), Sb-II and Rb-IV (K-III;[17] guest atoms smaller spheres, host atoms larger spheres). Crystallographic unit cells are indicated by gray lines. Projections are oriented along the *c* axes.

Despite the different interatomic distances within the germanium framework, each of the short Ge–Ge contacts in the crystal structure has its own attractor in ELI (Figure 6). This finding clearly confirms the directional character of the bonding. The positioning of the four maxima around the Ge2 atoms reflects a topological situation similar to that of Ge(*cF*8). Although the configuration of ELI around Ge1 is different, an additional maximum on the longer Ge1–Ge1 contact is not observed. In other words, the Ge1 atom exhibits (3+1+1) next-neighbor contacts while forming only four covalent bonds.

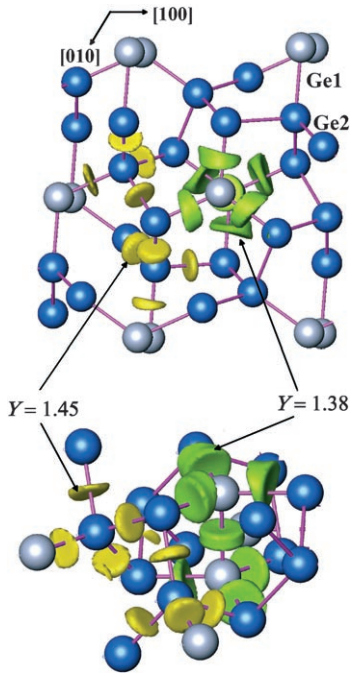

Figure 6. Isosurfaces of the electron localizability indicator *Y* for Ge(*hR*8). Top: view along [001]; bottom: view along [010]. Maxima of ELI clearly reveal the four-bonded character of both types of germanium atoms.

In summary, the structural organization of the new germanium allotrope bears some similarity to that of several recently described incommensurate high-pressure host–guest assemblies of elemental metals. However, both germanium atoms adopt the same bonding topology, which results in equivalent interactions within and between the partial structures of Ge(*hR*8). The covalent character of the bonds interconnecting network "host" and channel "guest" atoms stabilizes the commensurate order of this arrangement.

Experimental Section

The prepared germanium with clathrate as a main phase contained traces of sodium (0.34 wt%), oxygen (1.1 wt%), and hydrogen (0.27 wt%). A detailed discussion of contaminations can be found in references [4, 22]. The modification Ge(*tP*12) was synthesized from 99.9999% semiconductor-grade germanium in a multianvil device at 10(1) GPa and 1000(100) K. For the in situ high-pressure experiments, powdered samples were placed in steel gaskets using methanol/ethanol 4:1 as a pressure-transmitting medium. The diamond anvil cells for generating high pressures had culet sizes of typically 0.4 mm. Pressures were determined by the ruby luminescence method.[23]

X-ray powder diffraction measurements at high pressure were performed at the undulator beamline ID 09 A of the European Synchrotron Radiation Facility (ESRF, Grenoble). A bent Si(111) monochromator was used to select radiation of $\lambda = 0.413$ Å from the white (pink) beam. During exposure, samples were oscillated by $\pm 3°$ to enhance powder statistics. Intensities were recorded with imaging plates. For calibration of detector distance and wavelength we used a standard silicon sample, Si(*cF*8). Integration of the two-dimensional diffraction patterns was performed with the Fit2d software.[24] The crystal structure was refined using the data of isotypic Si(*hR*8) as starting values in the full-profile method. In the least-squares procedures performed with the program Fullprof,[25] we fixed the isotropic displacement factor to $B_{iso} = 1$ Å^2. In case of weak intensity contributions of phases, refinements were restricted to optimization of lattice parameters. Supplementary diffraction experiments were carried out in Debye–Scherrer geometry with MoK_α radiation. The ambient-pressure volume of Ge(*cF*136) was determined with Cu$K_{\alpha 1}$ radiation using a focusing setup (Huber Image Plate Guinier Camera G670) and LaB_6 as an internal standard. Diffraction data up to $2\theta = 100°$ were evaluated with the software WinCSD.[26] Equations of state were obtained by least-squares fits of Murnaghan-type functions to the experimental data.[27]

Electronic structure calculation and bonding analysis was carried out using the TB-LMTO-ASA program package.[28] The Barth–Hedin exchange potential[29] was employed for the LDA calculations. The radial scalar-relativistic Dirac equation was solved to get the partial waves. The calculation within the atomic sphere approximation (ASA) included corrections for the neglect of interstitial regions and partial waves of higher order; an addition of empty spheres was necessary. The following radii of the atomic and empty spheres were applied: r(Ge1) = 1.398 Å, r(Ge2) = 1.398 Å, r(E1) = 1.065 Å, r(E2) = 1.024 Å. A basis set containing Ge(4s,4p) orbitals was employed for a self-consistent calculations, with Ge(4d) functions being downfolded. The electron localizability indicator (ELI, *Y*) was evaluated according to reference [30] with an ELI module implemented within the TB-LMTO-ASA package. The topology of ELI was analyzed using the program Basin.[31]

Received: February 25, 2008
Revised: May 8, 2008
Published online: July 31, 2008

Keywords: allotropy · chemical bonding · germanium modification · host–guest systems

[1] "New materials and performance limits for thermoelectric cooling": G. A. Slack in *Handbook of Thermoelectrics* (Ed.: D. M. Rowe), CRC, Boca Raton, **1995**, p. 407.

[2] S. Paschen, W. Carrillo-Cabrera, A. Bentien, V. H. Tran, M. Baenitz, Yu. Grin, F. Steglich, *Phys. Rev. B* **2001**, *64*, 214404.

[3] A. Grüttner, R. Nesper, H. G. von Schnering, *Angew. Chem.* **1982**, *94*, 933; *Angew. Chem. Int. Ed. Engl.* **1982**, *21*, 912.

[4] A. Guloy, R. Ramlau, Z. Tang, W. Schnelle, M. Baitinger, Yu. Grin, *Nature* **2006**, *443*, 320.

[5] F. P. Bundy, J. S. Kasper, *Science* **1963**, *139*, 340; C. H. Bates, F. Dachille, R. Roy, *Science* **1965**, *147*, 860; J. S. Kasper, S. M. Richards, *Acta Crystallogr.* **1964**, *17*, 752; A. Wosylus, Yu. Prots, W. Schnelle, M. Hanfland, U. Schwarz, *Z. Naturforsch. B* **2008**, *63*, 608.

[6] R. J. Nelmes, M. I. McMahon, N. G. Wright, D. R. Allen, J. S. Loveday, *Phys. Rev. B* **1993**, *48*, 9883.

[7] C. S. Menoni, J. Z. Hu, I. L. Spain, *Phys. Rev. B* **1986**, *34*, 362.

[8] R. J. Nelmes, H. Liu, S. A. Belmonte, J. S. Loveday, M. I. McMahon, D. R. Allan, D. Häusermann, M. Hanfland, *Phys. Rev. B* **1996**, *53*, R2907.

[9] Y. K. Vohra, K. E. Brister, S. Desgreniers, A. L. Ruoff, K. J. Chang, M. L. Cohen, *Phys. Rev. Lett.* **1986**, *56*, 1944.

[10] K. Takemura, U. Schwarz, K. Syassen, M. Hanfland, N. E. Christensen, D. L. Novikov, I. Loa, *Phys. Rev. B* **2000**, *62*, R10603.

[11] The synthesis was performed in analogy to the given reference with $MgCl_2$ and *n*-dodecyltrimethylammonium chloride as HCl source at 550 K for 12 days; B. Böhme, A. Guloy, Z. Tang, W. Schnelle, U. Burkhardt, M. Baitinger, Yu. Grin, *J. Am. Chem. Soc.* **2007**, *129*, 5348.

[12] M. W. Guinan, D. J. Steinberg, *J. Phys. Chem. Solids* **1974**, *35*, 1501; K. A. Gschneidner, *Solid State Phys.* **1964**, *16*, 275.

[13] F. M. Walters, C. Wells, *Trans. Am. Soc. Met.* **1935**, *23*, 727; U. Zwicker, E. Jahn, K. Schuber, *Z. Metallkde* **1949**, *40*, 433; S. Setz, H. Nowotny, F. Benesovsky, *Monatsh. Chem.* **1968**, *99*, 730; J. A. Oberteuffer, J. A. Ibers, *Acta Crystallogr. Sect. B* **1970**, *26*, 1499; R. Benz, J. F. Elliott, J. Chipman, *Metall. Trans.* **1973**, *4*, 1449; A. Cely, L. E. Tergenius, T. Lundstöm, *J. Less-Common Met.* **1978**, *61*, 193.

[14] J. C. Jamieson, *Science* **1963**, *140*, 72.

[15] U. Schwarz, K. Takemura, M. Hanfland, K. Syassen, *Phys. Rev. Lett.* **1998**, *81*, 2711.

[16] M. Hanfland, U. Schwarz, K. Syassen, K. Takemura, *Phys. Rev. Lett.* **1999**, *82*, 1197; U. Schwarz, K. Syassen, A. Grzechnik, M. Hanfland, *Solid State Commun.* **1999**, *112*, 319.

[17] U. Schwarz, L. Akselrud, H. Rosner, A. Ormeci, Yu. Grin, M. Hanfland, *Phys. Rev. B* **2003**, *67*, 214101; M. I. McMahon, R. J. Nelmes, U. Schwarz, K. Syassen, *Phys. Rev. B* **2006**, *74*, 140102.

[18] For recent reviews, see U. Schwarz, *Z. Kristallogr.* **2004**, *219*, 376; M. I. McMahon, *Z. Kristallogr.* **2004**, *219*, 742; original contributions: U. Schwarz, A. Grzechnik, K. Syassen, I. Loa, M. Hanfland, *Phys. Rev. Lett.* **1999**, *83*, 4085; M. I. McMahon, S. Rekhi, R. J. Nelmes, *Phys. Rev. Lett.* **2001**, *87*, 055501; M. I. McMahon, T. Bovornratanaraks, D. R. Allen, S. A. Belmonte, R. J. Nelmes, *Phys. Rev. B* **2000**, *61*, 3135; R. J. Nelmes, D. R. Allan, M. I. McMahon, S. A. Belmonte, *Phys. Rev. Lett.* **1999**, *83*, 4081; M. I. McMahon, O. Degtyareva, R. J. Nelmes, *Phys. Rev. Lett.* **2000**, *85*, 4896; H. Fujihisa, Y. Akahama, H. Kawamura, Y. Gotoh, H. Yamawaki, M. Sakashita, S. Takeya, K. Honda, *Phys. Rev. B* **2005**, *72*, 132103; M. I. McMahon, L. F. Lundegaard, C. Hejni, S. Falconi, R. J. Nelmes, *Phys. Rev. B* **2006**, *73*, 134102.

[19] H. Bärnighausen, *Math. Chem.* **1980**, *9*, 139.

[20] R. O. Piltz, J. R. Maclean, S. J. Clark, G. J. Ackland; P. D. Hatton, J. Crain, *Phys. Rev. B* **1995**, *52*, 4072; P. D. Hatton, J. Crain, *Phys. Rev. B* **1995**, *52*, 4072.

[21] M. Kohout, K. Pernal, F. R. Wagner, Yu. Grin, *Theor. Chem. Acc.* **2004**, *112*, 453.

[22] A recent NMR investigation of the silicon clathrate Cs_8Si_{136} reveals that hydrogen is adsorbed at the surface and not incorporated into the bulk material; I. Veremchuck, F. Haarmann, T. Goebel, R. Ramlau, S. Hoffman, W. Schnelle, M. Baitinger, Yu. Grin, unpublished results.

[23] G. J. Piermarini, S. Block, J. D. Barnett, R. A. Forman, *J. Appl. Phys.* **1975**, *46*, 2774; H. K. Mao, P. M. Bell, J. W. Shaner, D. J. Steinberg, *J. Appl. Phys.* **1978**, *49*, 3276.

[24] A. Hammersley, Computer program Fit2d, ESRF, Grenoble, **1996**; A. P. Hammersley, S. O. Svenson, M. Hanfland, A. N. Fitch, D. Häusermann, *High Pressure Res.* **1996**, *14*, 235–248.

[25] J. Rodriguez-Carvajal, *Physica B* **1993**, *192*, 55.

[26] L. G. Akselrud, P. Y. Zavalij, Yu. Grin, V. K. Pecharsky, B. Baumgartner, E. Wölfel, *Mater. Sci. Forum* **1993**, *133–136*, 335.

[27] F. D. Murnaghan, *Proc. Natl. Acad. Sci. USA* **1944**, *30*, 244.

[28] O. K. Andersen, *Phys. Rev. B* **1975**, *12*, 3060; O. Jepsen, A. Burkhardt, O. K. Andersen, The TB-LMTO-ASA Program, Version 4.7. Max-Planck-Institut für Festkörperforschung, Stuttgart, **1999**.

[29] U. Barth, L. Hedin, *J. Phys. C* **1972**, *5*, 1629.

[30] M. Kohout, *Int. J. Quantum. Chem.* **2004**, *97*, 651.

[31] M. Kohout, BASIN. Version 2.3. Max-Planck-Institut für Chemische Physik fester Stoffe, Dresden, **2001**.

